Available online at www.sciencedirect.com
ScienceDirect
Vacuum 80 (2006) 1161–1166
VACUUM
SURFACE ENGINEERING, SURFACE INSTRUMENTATION & VACUUM TECHNOLOGY
www.elsevier.com/locate/vacuum

Evaluation of plume characteristics of arc-heaters with various oxygen injection systems

Makoto Matsui[a,*], Tomoyuki Ikemoto[a], Hiroki Takayanagi[b], Kimiya Komurasaki[a], Yoshihiro Arakawa[b]

[a]Department of Advanced Energy, The University of Tokyo, 5-1-5 Kashiwanoha, Kashiwa, Chiba 277-8583, Japan
[b]Department of Aeronautics and Astronautics, The University of Tokyo, 7-3-1 Hongo, Bunkyo, Tokyo 113-8656, Japan

Abstract

Arc-heater plumes generated by various oxygen injection systems were investigated by laser absorption spectroscopy. Firstly, oxygen was directly injected into a high-temperature cathode-jet region through a thoriated-tungsten hollow cathode. Although number density of atomic oxygen was increased, erosion of the cathode was too severe to maintain stable discharge. Then, zirconium was used as a cathode material to reduce cathode erosion by oxidation. As a result, stable discharge was maintained for 3 h with pre-mixed argon–oxygen injection and number density of atomic oxygen was successfully increased.

Keywords: Arc-heater; Atomic oxygen; Zirconium cathode; Laser absorption spectroscopy

1. Introduction

Atomic oxygen sources have been used in various research fields such as material processing [1], plasma etching and ashing for semiconductor [2], oxidation of nuclear waste [3], developments of thermal protection system for reentry vehicles [4] and protection of satellites structure in low earth orbit against degradation [5]. Various plasma devices have been developed to produce atomic oxygen as tabulated in Table 1. An arc-heater is one of the promising generators because of its high flux density as well as its high particle speed, high temperature and large flow area with uniformity. It can reduce experimental time dramatically; for example, deposition rate is enhanced more than one order higher than conventional CVD/PVD plasma sources [6] or fluence of incident atomic oxygen to satellites with 1-year stay in low earth orbit can be simulated in less than a few decade minutes [7].

In our previous research, however, it was found that degree of dissociation in oxygen was much lower than that expected [8]. Fig. 1 shows a cross-section of conventional oxygen injection system. Oxygen is injected at the constrictor part separately from an inert working gas to prevent the cathode from oxidation.

Owing to this flow configuration, oxygen was neither enough mixed with the working gas nor dissociated in the constrictor region as schematically shown in Fig. 1. Although the oxygen was mixing in the plume, the dissociation rate was quite small because of the decrease in temperature, resulting in the low degree of dissociation in oxygen. In order to promote mixing, bi-throat anode design has been proposed [9].

In this study, arc-heaters with two kinds of oxygen injection systems were developed and their performances were evaluated by laser absorption spectroscopy.

2. Experimental method and apparatus

2.1. Laser absorption spectroscopy

Laser absorption spectroscopy is applicable to optically thick plasma and does not require absolute calibration using a calibrated light source or a density reference cell. In addition, measurement system using a diode laser can be portable [12,13].

*Corresponding author. Fax: 04 7136 8583.
E-mail address: matsui@al.t.u-tokyo.ac.jp (M. Matsui).

0042-207X/$ - see front matter © 2006 Elsevier Ltd. All rights reserved.
doi:10.1016/j.vacuum.2006.01.051

Table 1
Atomic oxygen generators

	Flux density ($cm^{-2}s^{-1}$)	Energy (eV)	Mach number	Operational time
Arcjet [9]	$\sim 10^{19}$	~0.6	~3	~hour
Laser detonation [10]	$\sim 10^{14}$	~4.6	>5	~μs (pulse)
Plasma processing [11] (ICP, ECR, SWP, HWP)	$\sim 10^{15}$	<0.1	Stationary	>day

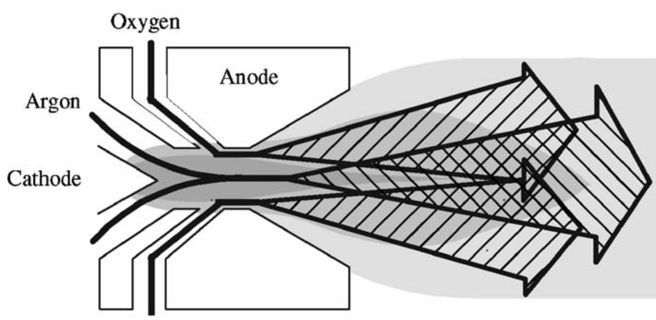

Fig. 1. Schematic of conventional oxygen injection and mixing process.

The relationship between laser intensity $I(\nu)$ and absorption coefficient $k(\nu, x)$ is expressed by the Beer–Lambert law as

$$\frac{dI(\nu)}{dx} = -k(\nu, x)I(\nu). \quad (1)$$

Here, ν is the laser frequency and x is the coordinate in the laser pass direction. Because distributions of absorption properties in plumes would be axisymmetric, local absorption coefficient $k(\nu, r)$ is obtained by the Abel inversion.

In our experimental conditions, Doppler broadening is several gigahertzes, which is two orders of magnitude greater than all other broadenings, including natural, pressure and Stark broadenings [13]. The absorption profile $k(\nu, r)$ is approximated as a Gaussian profile, expressed as

$$k(\nu, r) = \frac{2K(r)}{\Delta\nu_D}\sqrt{\frac{\ln 2}{\pi}}\exp\left[-\ln 2\left\{\frac{2(\nu-\nu_0)}{\Delta\nu_D}\right\}^2\right]. \quad (2)$$

Here, ν_0 is the center absorption frequency and $K(r)$ is the integrated absorption coefficient. $\Delta\nu_D$ is the full-width at half-maximum of the profile and is related to the translational temperature T, expressed as

$$\Delta\nu_D = 2\nu_0\sqrt{\frac{2k_B T}{mc^2}\ln 2}, \quad (3)$$

where m, c and k_B represent the mass of absorbers, velocity of light, and the Boltzmann constant, respectively.

Assuming Boltzmann relation between absorbing and excited states, integrated absorption coefficient is expressed as a function of the number density at the absorbing state $n_i(r)$ as

$$K(r) = \int_{-\infty}^{\infty} k_\nu(r)d\nu = \frac{\lambda^2}{8\pi}\frac{g_j}{g_i}A_{ji}n_i(r)\left[1 - \exp\left(-\frac{\Delta E_{ij}}{k_B T_{ex}}\right)\right]. \quad (4)$$

Here, subscripts 'i' and 'j' denote the absorbing and excited states, respectively. λ, g, A, ΔE and T_{ex} are the absorption wavelength, statistical weight, Einstein coefficient, energy gap between the states and electronic excitation temperature, respectively. Transition data of target absorption lines (OI 777.19 nm, ArI 842.46 nm) are referred in Ref. [14]. $\Delta E_{ij}/kT_{ex}$ was so large in the plumes that stimulated emission can be neglected and Eq. (4) is approximated as

$$K(r) = \frac{\lambda^2}{8\pi}\frac{g_j}{g_i}A_{ji}n_i(r). \quad (5)$$

2.2. Measurement system

The block diagram of measurement system is shown in Fig. 2. A tunable diode-laser with an external cavity was used as a probe and an etalon, whose free spectral range is 1 GHz, was used as a wavemeter. Probe beam was lead to a window of vacuum chamber through a multimode optical fiber. The fiber output was mounted on a one-dimensional traverse stage to scan the plume in the radial direction. At the other side of the chamber, the probe beam was focused on a photo-detector using a parabola mirror. This setup is possible to detect the probe beam without synchronizing the detector position with the laser scanning.

2.3. Arc-heaters and test conditions

2.3.1. Hollow injection

In this study, two kinds of oxygen injection system were developed. Firstly, instead of a conventional rod-shaped cathode, a hollow cathode was tested using thoriated-tungsten as cathode material. Oxygen is supplied through the cathode tip so as that oxygen passes through a high temperature cathode-jet region as shown in Fig. 3. The operating condition of the arc-heater is listed in Table 2. Compared with the conventional oxygen injection, oxygen flow rate at which arc discharge was sustainable was decreased by one-fifth.

2.3.2. Pre-mixed injection

Next, zirconium was used as cathode material instead of thoriated-tungsten to supply oxygen pre-mixed with argon